THE ASTRONOMICAL JOURNAL VOLUME 108, NUMBER 3 SEPTEMBER 1994

HIGH FREQUENCY VLA OBSERVATIONS OF LOW-REDSHIFT QUASARS: CORE STRUCTURE, VARIABILITY, AND ORIENTATION

MATTHEW L. LISTER[1] AND ANN C. GOWER

Department of Physics and Astronomy, University of Victoria, P.O. Box 3055, Victoria, BC V8W 2Y2, Canada
Electronic mail: lister@bu-ast.bu.edu, agower@otter.phys.uvic.ca

J. B. HUTCHINGS

Dominion Astrophysical Observatory, National Research Council of Canada, 5071 West Saanich Road, Victoria, BC V8X 4M6, Canada
Electronic mail: hutchings@dao.nrc.ca

Received 1994 March 2; revised 1994 April 26

ABSTRACT

We discuss high-frequency radio maps of 33 low-redshift quasars, taken with the VLA[2] (Very Large Array) in the A-configuration, at 1.3, 2, and 6 cm. In six sources we report the detection of new detailed structure. The 6 cm data are second-epoch observations and are used in discussion of core variability. Core variability is found to be present in both lobe- and core-dominated sources, with 12 quasars displaying significant flux changes over the two epochs. The majority of variable sources have flat or positive spectral indices, in agreement with other recent variability studies. We also consider the core fraction distribution of our sample of 114 quasars to redshift 2. This quantity does not correlate with source bend-angle or lobe length ratio as might be expected if the core flux is enhanced due to beaming when the source is aligned close to the line of sight. We confirm the correlation with apparent size, with a few exceptions, and show that these results are consistent with a source evolution scenario discussed in earlier papers.

1. INTRODUCTION

In a series of papers [Gower & Hutchings 1984a (GH); Hutchings *et al.* 1988 (HPG); Neff *et al.* 1989 (NHG); Neff & Hutchings 1990 (NH)] we have investigated the properties of radio quasars over a series of redshift intervals up to $z=3.7$. In this paper we present second-epoch observations of the low-redshift sample described in GH. We also investigate the core fraction statistics for the classical "triple" (lobe–core–lobe) sources in the combined sample with $z<2$.

The original GH sample consisted of nearly all of the radio loud quasars in the Hewitt & Burbidge (1980) catalogue having $z<0.3$ and declinations greater than $-25°$ (the lower limit of the VLA). Three objects with redshifts slightly greater than 0.3 were also included as their optical structure was known.

The first-epoch snapshot observations, made in 1982 April at 6 and 20 cm with the VLA in A-configuration, revealed a variety of source types, including core-dominated, one-sided, and double-lobed morphologies. Several sources also contained curved structure near the core that was just resolved at 6 cm. This made accurate determinations of the core fluxes and spectral indices difficult in these cases, and higher resolution data were needed to resolve the small-scale structure. Thus, the new observations were made at 2 cm. To obtain spectral index information it was also necessary to reobserve at 6 cm, since the cores of many of the sources were either known or thought to be variable. These second-epoch observations thus had the additional advantage of providing a variability measure for the whole sample.

There have been very few variability studies of the core components of extended radio quasars in the literature, primarily as a result of observational scheduling and time constraints. To resolve the core from the extended structure in double-lobed sources requires the sensitivity and large baselines provided by an interferometer, but these instruments have not often been used for long-term monitoring studies. The traditional approach has been to take regular flux-density measurements of a sample of sources over long time intervals with single-dish telescopes, thereby building up well sampled light curves. The poorer sensitivity of single dish instruments however has limited observations to relatively bright quasars only. Furthermore, in the case of extended, lobe-dominated sources, the large beam size blends the flux from core and extended structure, making core variability more difficult to detect.

Although our two epoch data cannot provide much information on the variability characteristics of individual sources, the sample is unique in that it contains both weak and strong sources, as well as core- and lobe-dominated objects. Furthermore, the maps are of sufficiently high resolution that the contributions from extended emission are greatly reduced.

2. OBSERVATIONS AND DATA REDUCTION

The observations were made by ACG in 1984, November, using the A-configuration of the VLA at 4.89 and 14.97 GHz (6 and 2 cm), with a bandwidth of 50 MHz. Additional ob-

[1]Present Address: Department of Astronomy, Boston University, 725 Commonwealth Ave. Boston, MA 02215.
[2]The VLA is operated by Associated Universities Inc. under cooperative agreement with the National Science Foundation.

 0004-6256/94/108(3)/821/7/$0.90

servations at 22.48 GHz (1.3 cm) were made for selected bright objects with possible small-scale structure near the core. Of the original 40 GH sources, 6 were not reobserved either due to the fact that no core was detected in the first-epoch 6 cm data, or due to scheduling constraints.

In order to maximize the coverage of the uv plane, two scans of approximately ten minutes were made for each object, separated by two hours in hour angle. Due to a snowstorm near the the end of the observing run, a substantial fraction of the sources was reobserved at later dates. These make-up observations were done in exactly the same manner, using the same array configuration and wavelength bands. At 6 and 2 cm the standard sources 3C 286 and 1803+784 were used as flux calibrators: the former source was not used for the 1.3 cm data as its small-scale structure is resolved in this configuration.

The images were analyzed with the Astronomical Image Processing System (AIPS) package following the same procedures described in HPG. In Table 1 we list the core fluxes and other derived quantities for the sample. As in our other papers, we adopt values of $H_0=100$ km s^{-1} Mpc^{-1} and $q_0=0.5$ for our cosmological model.

Column (1): IAU source name.

Column (2): Optical redshift from the Hewitt & Burbidge (1989) catalog.

Column (3): Source morphology, where C=core and L=lobe in increasing order of flux at 20 cm.

Column (4): Second-epoch observation date. The first epoch was 1982 April.

Columns (5–8): Core fluxes in milliJanskys. These were obtained using the JMFIT task in the AIPS package, which fits a two-dimensional Gaussian profile to the radio core component. In several sources the 2 cm data revealed small core extensions that were just resolved at 6 cm, implying that the latter fluxes were contaminated by extended structure. These fluxes are marked with an asterisk (*).

Column (9): Core spectral index between 6 and 2 cm, where $S\propto\nu^{\alpha}$.

Column (10): Core fraction (ratio of core to total flux) at 6 cm. As discussed in HPG, the A-configuration of the VLA is not sensitive to the large extended structure found in many sources, and cannot therefore provide reliable estimates of total source fluxes. We thus obtained values of the core fraction for all sources by estimating total flux values from log S vs log ν plots of single dish fluxes taken from the literature. The core fractions of sources marked with a colon (:) are more uncertain due to scatter in the log S vs log ν plots that is probably due to source variability and/or observational errors. All core fractions have been converted to rest frame values using the core 6–2 cm spectral indices and a typical value of $\alpha=-0.8$ for the extended structure.

Column (11): Core luminosities are corrected for bandpass and have also been converted to the quasar rest frame using the 6–2 cm core spectral indices.

Column (12): 6 cm core variability index as defined by Edelson (1987):

$$\frac{|S_{1984}-S_{1982}|}{(S_{1984}+S_{1982})/2}.$$

Column (13): Variability flag, where V="variable" and PV="probably variable." In order to assess whether a flux change at 6 cm between the two epochs was significant for a particular object in our sample, we used a method employed by Gregorini *et al.* (1986).

If the fluxes at the two epochs are $S_1\pm\sigma_1$ and $S_2\pm\sigma_2$ where the σ's are the observational errors, then the standard error of the difference in fluxes $\sigma_{\Delta S}$ is $[(\sigma_1)^2+(\sigma_2)^2]^{1/2}$. The distribution of $\Delta S/\sigma_{\Delta S}$ values for our sample was approximately Gaussian, enabling us to determine the probability that a particular value of ΔS was due to observational error. Sources having $\Delta S\geq 3.29\sigma_{\Delta S}$ were deemed variable at the 99.9% confidence level, and those with $\Delta S\geq 2.58\sigma_{\Delta S}$ (the 99% confidence level) were deemed probably variable.

Due to the undersampled (two-epoch) flux data, we note that variability may have gone undetected in several of our sample objects, so we cannot establish any particular object as nonvariable.

We have taken the observational errors (σ) in the strong (>10 mJy) sources to be 5% of the core flux, except those with extended structure near the core (marked with asterisks in Table 1), whose errors were estimated to be 20%. For the weak sources, we have also assumed an error of 20%, which was the upper limit of the standard errors obtained from the Gaussian core fits.

2.1 Images and Comments on Individual Objects

General morphological descriptions of the objects in the low-redshift sample can be found in GH. In this section and in Fig. 1 we present the images for which new morphological detail was revealed by the higher resolution 2 and 1.3 cm data.

0041+119 and 0137+012

The 2 cm data revealed similar "horseshoe" structures in the northern lobes of these two sources. These may be signatures of jet precession, as Gower & Hutchings (1984b) have found evidence of this phenomenon in 0137+012, and 0041+119 displays wiggly structure in its southern lobe at 20 cm (GH).

1020−103

The northern lobe of this source is quite faint, and there is no counter lobe present on the opposite side of the core. The slight core extension to the southeast fails to show up on the 1.3 cm map, which is due either to it having a steep spectral index, or to higher noise level in this map. A steep spectral index would be expected if we are seeing evidence of a new extended component in this source. At present it is unclear whether the absence of a counter-lobe in core–lobe sources is a result of beaming or an alternating-ejection phenomenon. Higher resolution VLBI images would allow one to look for signs that this extension is in fact a new jet.

2247+140, 2328+167, 2355−082

These sources all have intrinsic sizes $\lesssim$2 kpc, and also display curved structure near their cores. Such structures have often been seen in high-resolution maps of other sources (e.g., 3C 43, 3C 309.1), and may be modeled interms of various mechanisms, e.g., ballistic precession (Gower *et al.* 1982), helical instabilities (Hardee 1987), or

TABLE 1. Radio core data.

1	2	3	4	5	6	7	8	9	10	11	12	13
Object	z	Type[a]	Obs. Date	Core Flux (mJy)				Spectral Index[b]	Core Fraction	Core Lum. log[W Hz^{-1}]	Var. Index[c]	Var. Flag[d]
				1.3 cm	2 cm	6 cm	6 cm (1982)	(6-2 cm)	6 cm	6 cm	6 cm	
0007+106	0.087	C	1984 Nov 24	2128	1432	590	470	0.81	1.00	24.64	0.23	PV
0017+257	0.284	CLL	1984 Nov 24	-	357	299	310	0.16	0.48	25.34	0.04	
0041+119	0.228	LLC	1984 Nov 24	-	18	20	17	-0.08	0.07	24.01	0.15	
0137+012	0.260	CLL	1984 Nov 24	-	163	178	150	-0.08	0.22	25.07	0.17	
0241+622	0.044	CL	1984 Nov 24	615	191	256	300	-0.27	0.66	23.72	0.16	
0736+017	0.191	CLL	1985 Mar 8	-	2769	1882	2240	0.35	1.00:	25.80	0.17	
0742+318	0.462	CLL	1985 Mar 8	-	604	656	640	-0.07	0.79	26.10	0.02	
0829+047	0.180	CLL	1985 Mar 8	-	1588	1065	656	0.36	0.94	25.51	0.48	V
0846+100	0.366	LCL	1985 Mar 8	-	7.4	5.6	6	0.25	0.03	23.80	0.07	
0952+097	0.298	LCL	1985 Mar 8	-	5.5	7.8	7	-0.32	0.04	23.85	0.11	
1004+130	0.240	CLL	1985 Mar 8	-	29	30	12	-0.04	0.06	24.23	0.87	PV
1020-103	0.197	CLL	1985 Jan 19	95	133	367*	330*	-0.92	0.85	25.22	0.11	
1028+313	0.177	CLL	1985 Jan 19	-	107	83	110	0.24	0.47	24.39	0.28	V
1203+011	0.104	C	1985 Jan 19	-	114	154	170	-0.27	1.00	24.24	0.10	
1217+023	0.240	CLL	1985 Jan 19	-	319	330	320	-0.03	0.66	25.27	0.03	
1223+252	0.268	LLC	1985 Jan 19	-	6.6	3.5	4	0.58	0.02	23.32	0.13	
1243-072	0.270	CLL	1985 Jan 19	-	977	869	1300	0.11	0.96	25.77	0.40	V
1302-102	0.286	CLL	1985 Jan 19	-	927	982	1185	-0.05	0.95	25.89	0.19	PV
1525+227	0.253	CL	1985 Jan 19	-	59	39	43	0.38	0.21	24.34	0.10	
1635+119	0.146	CLL	1984 Nov 24	-	8	36	17	-1.37	0.75	23.97	0.72	V
1721+343	0.206	CLL	1984 Nov 24	-	210	386	370	-0.56	0.50	25.25	0.04	
1725+044	0.296	CL	1984 Nov 24	-	597	634	730	-0.06	0.85	25.72	0.14	
1739+184	0.186	LLC	1984 Nov 24	-	13	32	25	-0.83	0.10	24.10	0.25	V
2135-147	0.200	LCL	1984 Nov 24	-	157	136	126	0.13	0.09	24.72	0.08	
2141+175	0.213	C	1984 Nov 24	-	904	918	280	-0.01	1.00	25.61	1.07	V
2201+315	0.297	CLL	1984 Nov 24	-	4247	3696	1500	0.13	1.00:	26.47	0.85	V
2217+08N	0.623	CLL	1984 Nov 24	-	28	27	27	0.03	0.14	24.93	0.00	
2217+08S	0.228	CLL	1984 Nov 24	-	9.1	12	7	-0.29	0.15	23.83	0.56	V
2247+140	0.237	CL	1984 Nov 24	480	394	1277*	1210*	-1.07	1.00	25.94	0.05	
2305+187	0.313	CLL	1984 Nov 24	-	46	70	81	-0.38	0.15	24.85	0.15	
2328+167	0.284	CL	1984 Nov 24	-	6.3	41*	25*	-1.70	0.60	24.68	0.48	
2331-240	0.048	C	1984 Nov 24	-	1346	1197	910	0.11	1.00	24.46	0.27	V
2355-082	0.211	CL	1984 Nov 24	-	41	89*	110*	-0.71	0.45	24.65	0.21	

Notes to TABLE 1

- All quantities calculated assuming $H_o = 100$ km s^{-1} Mpc^{-1} and $q_o = 0.5$

a - Source morphology, where C = core and L = lobe in order of increasing flux at 20 cm.

b - Spectral index calculated using $S \propto \nu^{\alpha}$

c - The variability index is defined as:

$$\frac{|S_{1984} - S_{1982}|}{(S_{1984} + S_{1982})/2}$$

d - Variability flag, where V = variable at 99.9% confidence level, PV = probably variable at 99% confidence level.

* - Core flux probably contaminated by nearby extended structure (see Section 2).

: - Core fraction uncertain due to flux errors and/or variability (see Section 2).

nonballistic precession (Conway & Murphy 1992).

3. CORE VARIABILITY

Currently the most widely accepted models for quasar and BL Lac variability involve shocked jets originating from the AGN core (Hughes *et al.* 1989; Marscher & Gear 1985). These models have been very successful in reproducing the random, flare-like behavior of well known variable sources such as BL Lac, OT 081, and 3C 279 (Hughes *et al.* 1990). An important aspect of these models is that they involve bulk relativistic flows at angles $\lesssim 30°-40°$ to the line of sight, which has the implication that relativistic beaming may play a role in the cores of strongly variable sources. Since beaming amplifies only the flux from the core component and not that of the extended emission, the ratio of core to total flux,

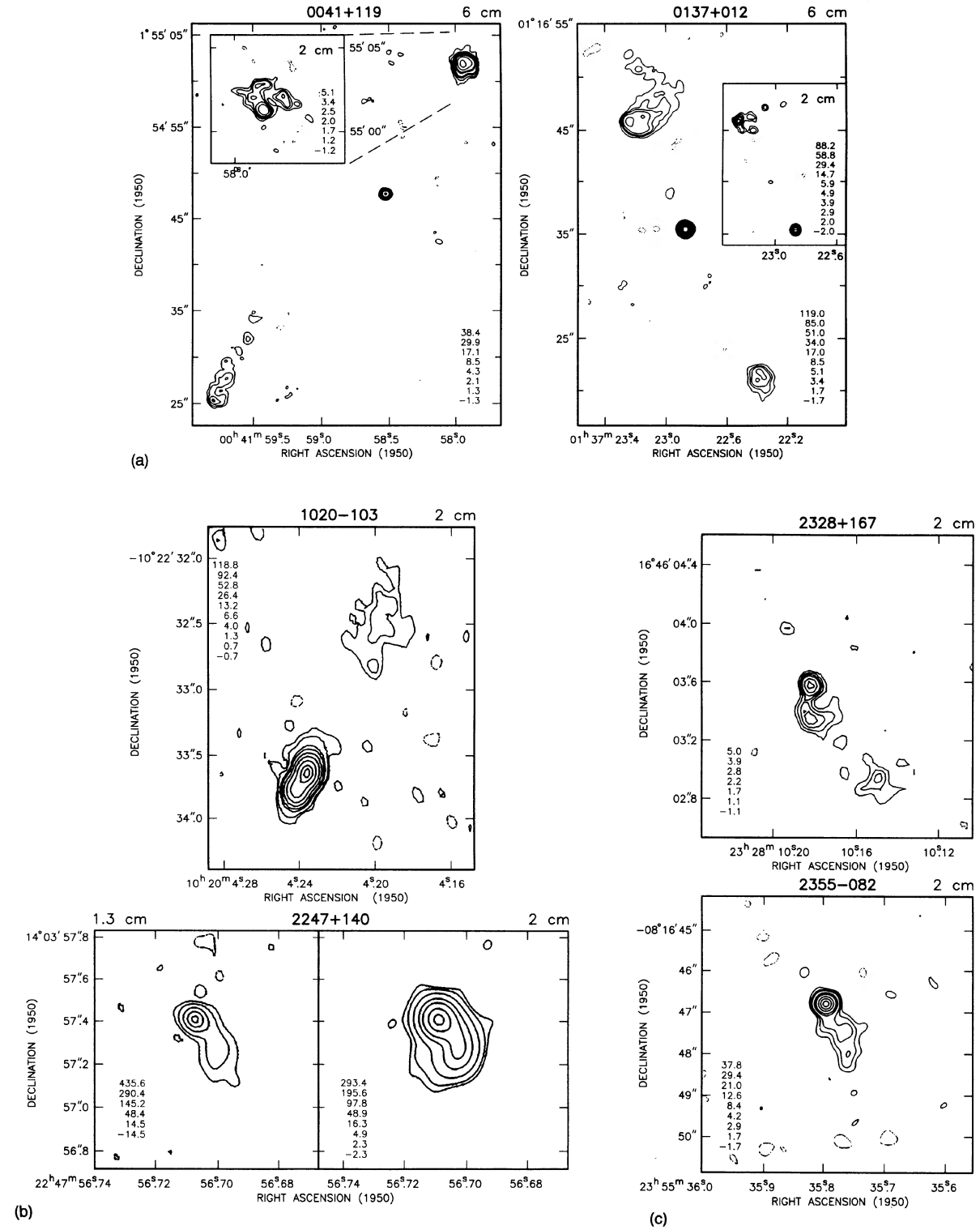

FIG. 1. Radio contour plots of selected objects in the GH sample for which new structure was detected at 2 cm. Contour levels are given in mJy/beam.

or core fraction, has been widely used as an indicator of beaming, and in turn, source orientation. Indeed, the core-dominated radio structure and strong variability of BL Lac objects has led to the suggestion that these may be highly beamed objects, viewed nearly along the jet axis (Ghisellini *et al.* 1993).

If the relativistic bulk flows in the cores of AGNs are aligned with the large scale structure, as is generally believed to be the case, then beamed sources, by virtue of being viewed "end-on," would not be expected to display classical triple morphologies. The core–halo radio morphology de-

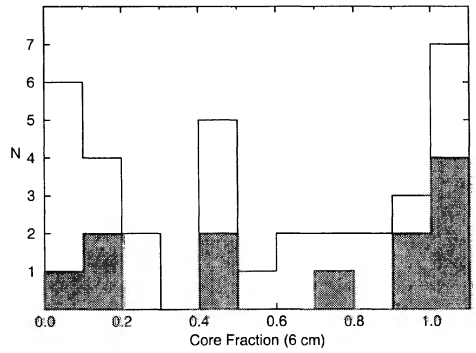

FIG. 2. Core fraction distribution for the sample, with variable and probably variable sources shaded.

tected in many of the BL Lac objects by Antonucci & Ulvestad (1985) is consistent with this hypothesis.

In Figs. 2 and 3 we show the core fraction and core luminosity distributions for our sample, with the variable and probably variable sources shaded. The variable sources show no tendency towards higher core fractions or luminosities, and are roughly evenly distributed within the sample ranges. Variability was also detected in both core- and lobe-dominated sources, as indicated in Table 2.

We conclude from these data that variability is a widespread phenomenon in our sample of low redshift quasars, and is not limited to any particular morphological class or luminosity range. This finding is in keeping with the results of optical monitoring programs, which show variability to be a defining characteristic of quasars. In order to fully investigate possible correlations between beaming and variability, more extensive monitoring of a larger sample of objects is required.

4. CORE VARIABILITY AND SPECTRAL INDEX

Several studies to date have found evidence that flat- and inverted-spectrum radio sources (including both radio galaxies and quasars) display more flux variability than steep

TABLE 2. Variability statistics by morphological class.

Morphology	Variable	Probably Variable	No Variability Detected
Core-Dominated	2	1	1
One-sided	0	0	6
Triple	7	2	14

spectrum ones (Aller 1991; Edelson 1987; Heeschen & Rickett 1987). Although this finding is extremely interesting in terms of trying to understand the mechanisms behind flux variability in quasars, it is also somewhat confusing as the spectral indices used in these authors' studies are derived from total fluxes (i.e., core+extended components). Since simple light-time travel arguments have led to the deduction that flux variability must originate in the cores of quasars, a correlation with *core* spectral index would be of much greater use.

In addition to this problem of core and total spectral index, the above studies also suffered from the problems associated with single dish telescopes: larger flux errors, and much lower sensitivity than interferometers such as the VLA. Also, in many cases the spectral indices were derived from flux measurements taken at different times, which can introduce large errors for variable sources.

In Fig. 4 we show the core spectral-index (between 6 and 2 cm) distributions of the sample, with the variable and probably variable sources shaded. The distribution for the entire sample closely resembles that of the quasars in the Pearson & Readhead (1988) sample, shown in Aller *et al.* (1992). The majority of variable sources have flat or positive spectral indices, in agreement with the latter paper.

In Fig. 5 we have plotted core luminosity at 6 cm vs the 6−2 cm spectral index. Among the variable cores, there are three which have steep ($\alpha<0$) spectral indices: 1635+119, 1739+184, and 2217+08*S*. It is interesting to note that these cores are also the weakest of all the variable sources in the sample. This may be indicative of intrinsic differences in the variability characteristics of weak cores, but the small

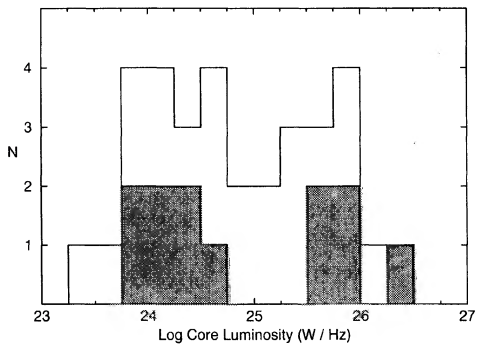

FIG. 3. Core luminosity distribution for the sample, with variable and probably variable sources shaded.

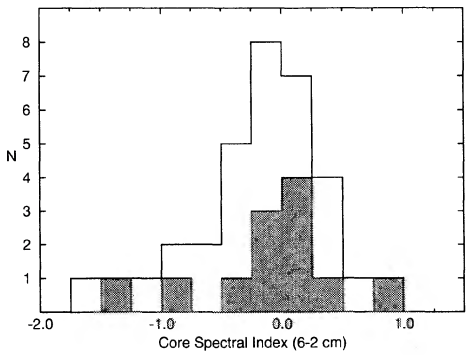

FIG. 4. Core spectral index distribution for the sample, with variable and probably variable sources shaded.

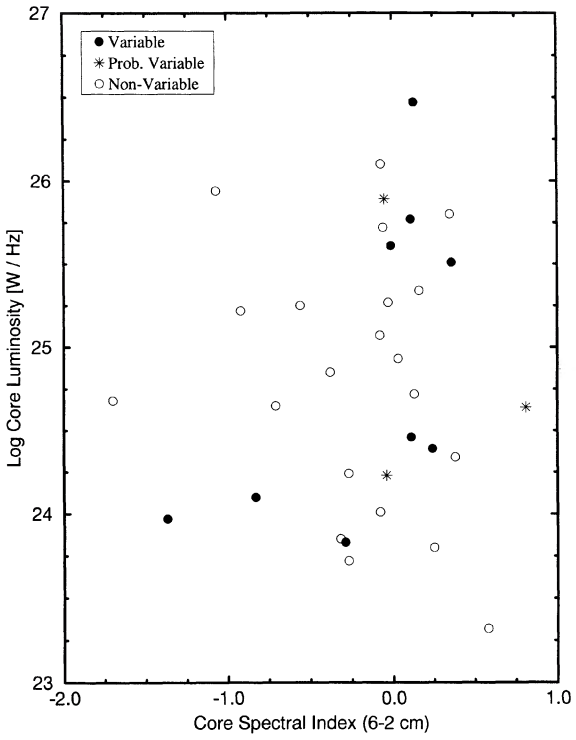

FIG. 5. Plot of core luminosity vs core spectral index for the sample, with variable cores shaded.

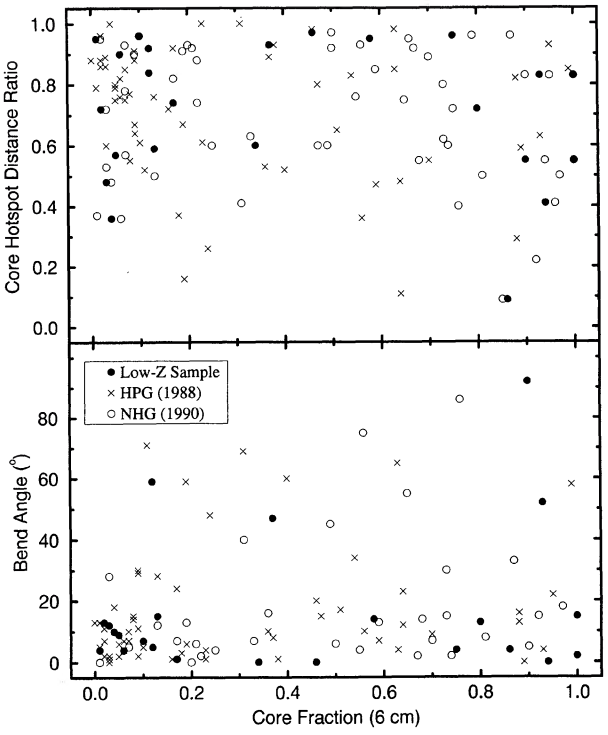

FIG. 6. Top panel: core-to-hot spot distance ratio vs core fraction for our sample sources along with additional triple quasars from the LHG sample. Lower panel: bend angle vs core fraction for the same sources.

number statistics limit the strength of this conclusion. To confirm this a much larger database is required.

5. SOURCE ORIENTATION AND CORE FRACTION

Our dataset provides us with a unique means of evaluating the merits of core fraction statistics as an orientation indicator, by looking for correlations with the apparent size, bend angle, and the ratio of core-to-hot spot distances of our sample objects. In a separate paper [Lister *et al.* 1994 (LHG)], we discussed how these latter three quantities are all affected by projection and foreshortening effects, and would thus all be expected to be related to the core fraction if it were an orientation indicator.

To improve our chances of detecting possible correlations, we have enlarged our database by including other quasars from the LHG sample. The LHG sample consists of 114 triple sources assembled from GH, HPG, and NHG, and was carefully chosen with no reference to source morphology or spectral index. Every attempt was made to sample the 2.7 GHz flux/redshift plane as widely as possible, and all sources lie between $0<z<2$, as it has been suggested (Barthel & Miley 1988) that the intrinsic properties of quasars evolve with redshift. Further details of the sample selection can be found in LHG, GH, HPG, and NHG.

In LHG we discussed how a quasar aligned close to the line of sight would be expected to have a large apparent bend angle and a core–hot spot distance ratio substantially less than unity due to unequal foreshortening of the lobes. If the core fraction is an orientation indicator, we would expect core fractions to increase with bend-angle and lobe-length asymmetry. In Fig. 6 we plot the apparent bend-angle and core–hot spot distance ratio against core fraction at 6 cm for the LHG sample. As the core fractions tabulated in HPG and NHG were not corrected to rest frame values, for this plot, we have corrected the low-z data to the values they would have at $z=1$. In fact our conclusions are not dependent on this correction, and Fig. 6 shows no evidence for a correlation between these two quantities and the core fraction. This suggests that the core fraction is not related to source orientation for the LHG sample.

In Fig. 7 we plot the apparent size of the LHG sources versus the core fraction at 6 cm. With the exception of the labeled sources, which we discuss below, there is a distinct upper envelope to the distribution, which was also noted by Kapahi & Saikia (1982) in a sample of 78 double-lobed quasars. The majority of sources with high core fractions tend to have small apparent sizes, which *is* in keeping with the predictions of the beaming model.

The labeled sources in Fig. 7(a) appear to have anomalously bright cores for their sizes. The core fractions of 1721+343, 0742+318, and 1217+023 are all in agreement with those previously obtained by Jägers *et al.* (1982) and Neff (1982). On the other hand, 2201+315 and 1635+119 are both highly variable sources, making their measured core fractions less certain. These sources may have a beamed core component that is misaligned with the large scale structure, or the core may have undergone a burst of reactivity following a recent merger event (Hutchings & Neff 1992). What-

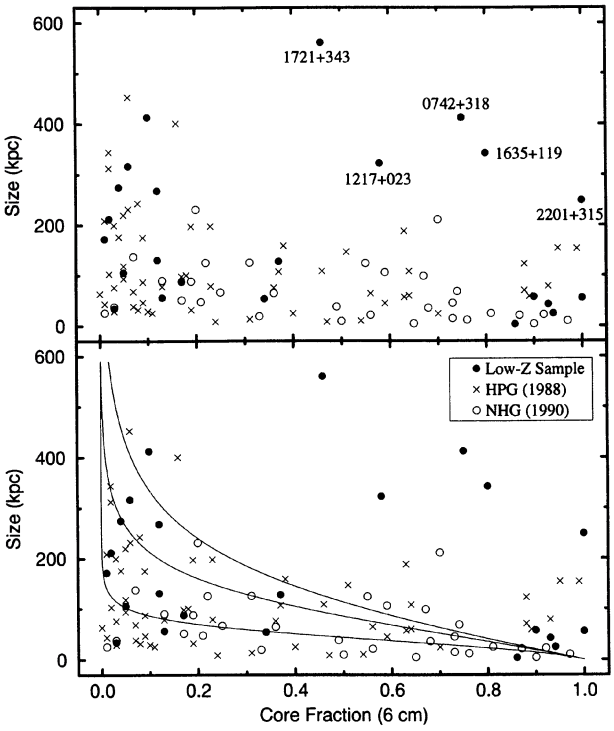

FIG. 7. Top panel: apparent size vs core fraction for our sample sources along with additional triple quasars from the LHG sample. The sources labeled appear to have anomalously bright cores for their linear sizes, the reasons for which are unclear. Lower panel: same data overlaid with possible evolutionary paths for a source which starts out as core dominated, and then grows lobes as its core luminosity decays with time. The curves shown differ only in the rate of exponential core decay.

ever their peculiarities, for the present discussion we regard them as atypical.

The lack of correlations in Fig. 6 and the upper envelope in Fig. 7(a) are both consistent with the evolutionary scheme for radio quasars described in HPG. In this model, sources start out as core dominated, and then develop increasingly larger radio lobes as the core fades. The core fraction and apparent size, being both functions of age, would therefore be correlated, and no correlation would be expected between the core fraction and the other two orientation indicators.

By adopting a simple model in which the core flux decays exponentially while the lobe flux grows linearly, evolutionary curves can be fit to the data as in Fig. 7(b). The family of curves shown differ only in the core decay rates. While there are no observational constraints on the free parameters in this model, Fig. 7(b) shows that it can be used quantitatively as an alternative to the beaming interpretation of the core fraction statistics, which does not seem to work.

6. CONCLUSIONS

(1) We find core structure at the 1 kpc level in three sources, and at the 3 kpc level in one source. We present images of kpc-scale structure near the cores of four low-redshift quasars, and in the lobes of two others.

(2) We find that 36% of the sources in our sample of 33 low-redshift quasars showed a significant change in core flux at 6 cm between 1982 and 1984. Variability was detected in three core dominated sources, zero one-sided sources, and nine triple sources. No trends with core fraction or luminosity were noted for the variable sources. Five sources were variable at the 20%–30% level, while the remaining seven variable sources were distributed roughly evenly between 30% and 110%.

(3) The spectral index distribution of cores is approximately Gaussian, with a peak at $\alpha=-0.25$. The overall distribution is similar to that of the Pearson and Readhead sample (Aller *et al.* 1992), and the majority of variable sources have flat or positive spectral indices.

(4) We find that the core fraction does not correlate with bend angle or core–hot spot distance ratio. The relation with size is consistent with both beaming and a simple source growth scenario. Thus it is not useful for determining source orientation, as it can be strongly affected by source evolution, relativistic beaming, and core–lobe misalignments.

(5) Continued observations of this type are needed to address these questions more quantitatively.

We wish to thank the referee for valuable and thoughtful suggestions. M.L.L. wishes to acknowledge a research grant from David Hartwick, Chris Pritchet, and Don VandenBerg of the University of Victoria.

REFERENCES

Aller, M. F. 1991, Variability of Active Galactic Nuclei, edited by H. Miller and P. Wiita (Cambridge University Press, Cambridge)
Aller, M. F., Aller, H. D., & Hughes, P. A. 1992, ApJ, 399, 16
Antonucci, R. J., & Ulvestad, J. S. 1985, ApJ, 294, 158
Barthel, P., & Miley, G. K. 1988, Nature, 333, 319
Conway, J., & Murphy, D. 1993, ApJ, 411, 89
Edelson, R. 1987, AJ, 94, 1150
Ghisellini, G., Padovani, P., Celotti, A., & Maraschi, L. 1993, ApJ, 407, 65
Gower, A. C., Gregory, P. C., Hutchings, J. B., & Unruh, W. G. 1982, ApJ, 262, 478
Gower, A. C., & Hutchings, J. B. 1984a, ApJ, 89, 1658 (GH)
Gower, A. C., & Hutchings, J. B. 1984b, PASP, 96, 19
Gregorini, L., Ficarra, L., & Padrielli, L. 1986, AJ, 168, 25
Hardee, P. E. 1987, ApJ, 318, 78
Heeschen, D., & Rickett, B. 1987, AJ, 93, 589
Hewitt, A., & Burbidge, G. 1980, ApJS, 43, 57
Hewitt, A., & Burbidge, G. 1989, ApJS, 69, 1
Hughes, P., Aller, H., & Aller, M. 1989, ApJ, 341, 54
Hughes, P., Aller, H., & Aller, M. 1990, in Parsec Scale Radio Jets, edited by J. A. Zensus and T. J. Pearson (Cambridge University Press, Cambridge), p. 250
Hutchings, J. B., & Neff, S. G. 1992, AJ, 104, 1
Hutchings, J. B., Price, R., & Gower, A. C. 1988, ApJ, 329, 122 (HPG)
Jägers, W., van Breugel, W., Miley, G., Schilizzi, R., & Conway, R. 1982, A&A, 105, 278
Kapahi, V. K., & Saikia, D. J. 1982, J. Astron. Astrophys., 3, 465
Lister, M. L., Hutchings, J. B., & Gower, A. C., 1994, ApJ, 427, 125 (LHG)
Marscher, A., & Gear, W. 1985, ApJ, 298, 114
Neff, S. 1982, Ph.D. thesis, University of Virginia
Neff, S. G., & Hutchings, J. B. 1990, AJ, 100, 1441 (NH)
Neff, S. G., Hutchings, J. B., & Gower, A. C. 1989, AJ, 97, 1291 (NHG)
Pearson, T. J., & Readhead, A. C. S. 1988, ApJ, 328, 114